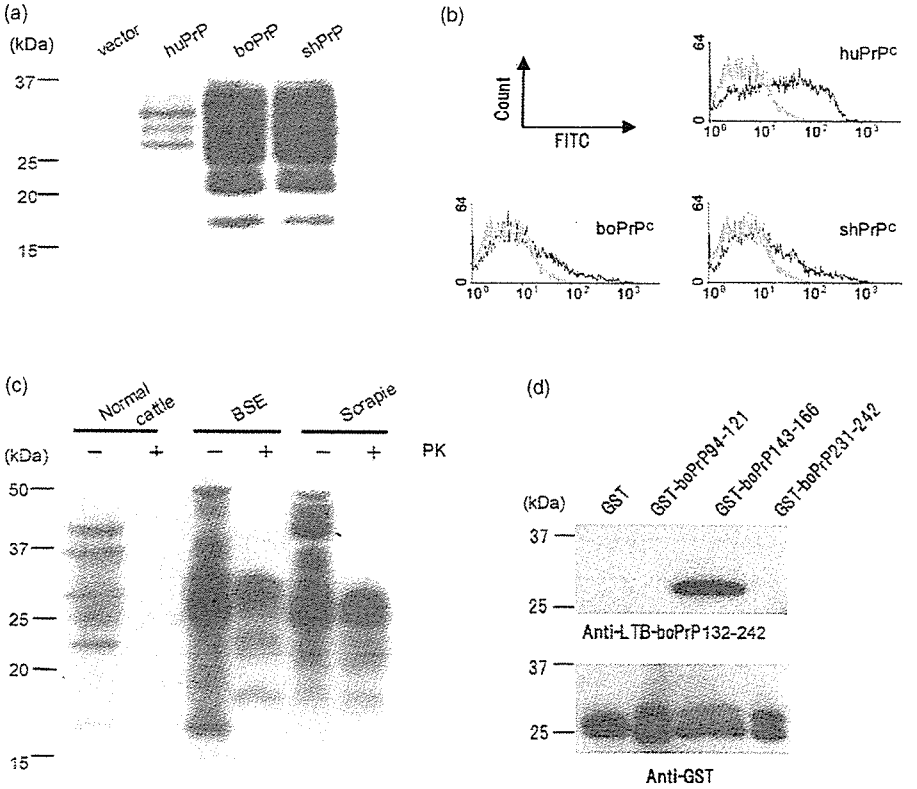

Fig. 3. Immunoblotting (a) and FACS analysis (b) of COS-7 cells expressing hu, bo, and shPrP^C with anti-LTB-boPrP132–242 sera. In (b), solid and gray lines indicate the cells transfected by a vector inserted with or without PrP cDNA, respectively. (c) Immunoblotting of the brains of normal and BSE-affected cattle and scrapie-affected sheep with anti-LTB-boPrP132–242 sera with (+) or without (−) treatment with proteinase K (PK). (d) Immunoblotting of GST-fused peptides of boPrP with anti-LTB-boPrP132–242 sera.

143–166 was substantially recognized with the sera (Fig. 3d), suggesting that immunization with LTB-boPrP132–242 could be prophylactic against BSE prions.

3.5. Anti-PrP autoantibodies in mice immunized with LTB-moPrP120–231 and LTB-boPrP132–242

To detect anti-moPrP IgG autoantibodies in Balb/c mice immunized with LTB-moPrP120–231 and LTB-boPrP132–242, we performed ELISA with these antisera against recombinant moPrP without a 6 × His tag. Mice were immunized six times at 2-week intervals. The mice immunized with moPrP120–231 could not elicit anti-PrP autoantibodies (Fig. 4a). However, immunization of mice with LTB-moPrP120–231 produced low but significantly higher titers of antibodies reactive with moPrP (Fig. 4a), indicating that fusion with LTB could break the tolerance of PrP only with very low efficiency. Similar or slightly lesser amounts of IgG cross-reactive with moPrP were observed in the mice immunized with boPrP132–242 but the fusion with LTB could not increase titers of the antibodies (Fig. 4b). Presumably due to low titers of the autoantibodies, we could not detect any specific reduction of PrP^{Sc} in the infected N2a cells treated with these antisera (data not shown).

4. Discussion

In the present study, we showed that fusion with LTB could markedly enhance the mucosal immunogenicity of boPrP132–242 in mice. Intranasal immunization with non-fused boPrP132–242 stimulated moderate antibody responses in Balb/c but not C57BL/6 mice. However, LTB-boPrP132–242 elicited very strong responses in both mouse strains, producing a marked increase in boPrP-specific IgA and IgG in serum. Specific secretory IgA was also abundantly observed in the intestines of the immunized mice.

The exact route of the orally ingested prions from the intestinal tract to the central nervous system is still uncertain. Accumulating evidence suggests that the ingested prions are transepithelially transported via M cells lining the intestinal membrane of Peyer's patches to the underlying follicular dendritic cells that are crucial for the prions to replicate and to reach the nervous system [19,20]. It was previously shown that certain monoclonal antibodies against PrP effectively prevented the infection of peripherally inoculated prions in mice, indicating that anti-PrP antibodies could neutralize prions invading the body [11–13]. IgA is a key player in pathogen-specific mucosal immunity. It is therefore feasible that anti-PrP IgA antibodies block the entry of

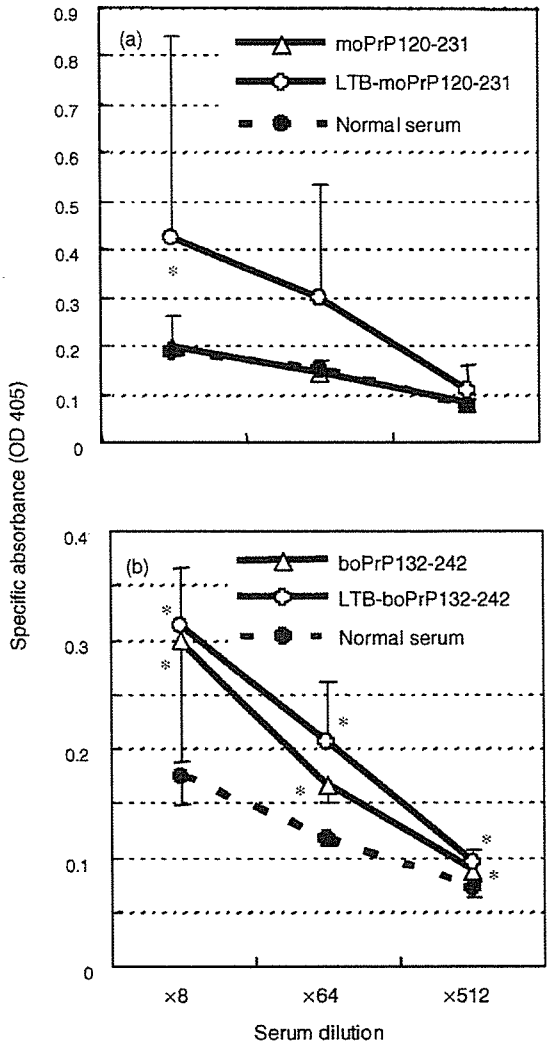

Fig. 4. Anti-moPrP autoantibodies in Balb/c mice immunized with mo (a) and boPrPs (b) fused with or without LTB, six times at 2-week intervals. Antisera were collected from four to five mice from each group and subjected to ELISA against moPrP without a 6 × His tag. Antibodies titers were expressed by colorimetric values at 405 nm. Data were analyzed using the Mann–Whitney *U*-test. Data were represented by mean ± S.D. $^{*}p < 0.05$.

orally ingested prions into the body. Intranasal immunization of mice with LTB-boPrP132–242 produced markedly higher titers of boPrP-specific IgG and IgA in sera irrespective of mouse strain genetic differences. We showed that the IgG antibodies could react with the putative anti-BSE prion epitope, strongly suggesting that these antibodies could neutralize BSE prions invading the body. We also showed that specific IgA was abundantly secreted in the intestines of these mice. It is therefore conceivable that orally-ingested BSE prions could be blocked at the intestinal entry point. Taken together, these results suggest that LTB-boPrP132–242 could be potent mucosal vaccines to prevent the transmission of prions from cattle to humans.

However, in nvCJD, the invading BSE prions convert endogenous human PrP^{C} into PrP^{Sc} upon the heterologous interaction with bovine PrP^{Sc}, and once human PrP^{Sc} is generated, the conversion effectively takes place via the syngeneic interaction of human PrP^{C} and human PrP^{Sc}. This constitutive syngeneic conversion of PrP results in fatal progression of the disease. To block the disease progression or to cure the disease, it is important to prevent the syngeneic interaction of human PrPs. Thus, boPrP-specific antibodies raised by LTB-boPrP132–242 vaccination probably have no therapeutic potential.

The prevalence of BSE within cattle is thought to be attributable to ingestion of BSE prion-contaminated food [21]. It is also recently reported that blood transfusion might be a risk factor for prion transmission in humans [22,23]. These urge the development of prophylactic measures against the intraspecies transmission of prions as well. However, individuals are tolerant to self-PrP. In fact, moPrP120–231 could barely evoke antibody responses in mice. However, fusion with LTB slightly but significantly induced IgG autoantibodies to moPrP in Balb/c mice, indicating that the fusion with LTB could circumvent the tolerance of PrP with very low efficiency. Intriguingly, immunization of mice with boPrP132–242 itself generated antibodies cross-reactive with moPrP with similar or slightly lower titers compared with those in LTB-moPrP120–231-immunized mice. In contrast to the case of moPrP120–231, fusion of boPrP132–242 with LTB could not enhance the production of cross-reactive antibodies in mice. These results suggest that immunization with heterologous recombinant PrPs themselves elicit autoantibodies in mice. It is therefore interesting to investigate whether or not immunization of mice with LTB-boPrP132–242 could be effective against the infections of mouse-adapted prions. If so, LTB-fused heterologous PrPs could be potential mucosal vaccines prophylactic against both the interspecies and the intraspecies transmission of prions.

Titers of the cross-reactive antibodies were very low in the mice immunized with LTB-fused boPrP132–242. Therefore, for vaccination with LTB-boPrP132–242 to be more effectively protective against the prion infection, it may be necessary to overcome B cell tolerance more efficiently. It was recently reported that oral vaccination with an attenuated *Salmonella typhimurium* strain expressing moPrP alone significantly delayed the disease in mice after inoculation of the mouse-adapted 139A scrapie prion, probably by eliciting autoantibodies against moPrP [24]. We showed here that mucosal vaccination of mice with LTB-fused moPrP120–231 or heterologous boPrP132–242 alone stimulated more production of anti-PrP autoantibodies than that of moPrP120–231 alone. It is therefore worthy to examine whether or not an attenuated *Salmonella typhimurium* strain expressing LTB-moPrP or heterologous PrPs could be more effective against the prion infection than one expressing moPrP alone. Molecular mimicry is a hypothetical mechanism for autoimmune diseases [25,26]. This hypothesis

postulates that shared identical amino acid sequences or homologous but non-identical amino acid sequences between microbial and host antigens could be essential for the initial processes of molecular mimicry, producing autoantibodies and/or auto-reactive T cells against the host antigens. Our results showing that heterologous boPrP was immunogenic inducing anti-PrP autoantibodies might be consistent with this hypothesis. Therefore, isolating molecules or peptides with much stronger antigenic mimicry to moPrP could be potentially important for prion vaccine development. It was reported that co-administration of moPrP with CpG-rich oligonucleotides, fusion of PrP with the heat shock protein DnaK, and dimerization of moPrP could break the tolerance and efficiently elicit autoantibodies against moPrP without inducing any autoimmune disease-specific symptoms in mice [27–29]. It is therefore interesting to investigate whether LTB-fused PrPs could increase the production of such cross-reactive antibodies either by co-administration with CpG or by such modifications of PrP. Nikes et al. recently showed that retrovirus-like particles (VLP) displaying the C-terminal 111 amino acids of moPrP fused with the transmembrane domain of the platelet-derived growth factor receptor could overcome B cell tolerance in mice to elicit anti-PrP autoantibodies able to react with native $moPrP^C$ [30]. It might also be interesting to investigate the immunogenicity of VPL displaying heterologous PrPs alone or LTB-fused heterologous PrPs. So far, no prion vaccines completely protective against prion infection have been developed. Further studies are required to determine how to circumvent B cell tolerance against PrP and induce much more antibodies protective against prion diseases.

Acknowledgements

We all thank Prof. Motohiro Horiuchi (Hokkaido University) for providing bovine PrP cDNA and brain tissues from BSE-affected cattle and scrapie-affected sheep. This study was supported in part by a Research on Specific Diseases grant from the Ministry of Health, Labour and Welfare, Japan.

References

[1] Prusiner SB. Prions. Proc Natl Acad Sci USA 1998;95:13363–83.
[2] Weissmann C, Enari M, Klohn PC, Rossi D, Flechsig E. Molecular biology of prions. Acta Neurobiol Exp (Wars) 2002;62:153–66.
[3] Will RG, Alperovitch A, Poser S, Pocchiari M, Hofman A, Mitrova E, et al. Descriptive epidemiology of Creutzfeldt-Jakob disease in six European countries. Ann Neurol 1998;43:763–7.
[4] Duffy P, Wolf J, Collins G, DeVoe AG, Streeten B, Cowen D. Letter: possible person-to-person transmission of Creutzfeldt-Jakob disease. N Engl J Med 1974;290:692–3.
[5] Bernoulli C, Siegfried J, Baumgartner G, Regli F, Rabinowicz T, Gajdusek DC, et al. Danger of accidental person-to-person transmission of Creutzfeldt-Jakob disease by surgery. Lancet 1977;1:478–9.
[6] Koch TK, Berg BO, De Armond SJ, Gravina RF. Creutzfeldt-Jakob disease in a young adult with idiopathic hypopituitarism. Possible relation to the administration of cadaveric human growth hormone. N Engl J Med 1985;313:731–3.
[7] Thadani V, Penar PL, Partington J, Kalb R, Janssen R, Schonberger LB, et al. Creutzfeldt-Jakob disease probably acquired from a cadaveric dura mater graft. Case report. J Neurosurg 1988;69:766–9.
[8] Bruce ME, Will RG, Ironside JW, McConnell I, Drummond D, Suttie A, et al. Transmissions to mice indicate that 'new variant' CJD is caused by the BSE agent. Nature 1997;389:498–501.
[9] Hill AF, Desbruslais M, Joiner S, Sidle KC, Gowland I, Collinge J, et al. The same prion strain causes vCJD and BSE. Nature 1997;389:448–50. 526.
[10] Prusiner SB. Molecular biology of prion diseases. Science 1991;252:1515–22.
[11] Gabizon R, McKinley MP, Groth D, Prusiner SB. Immunoaffinity purification and neutralization of scrapie prion infectivity. Proc Natl Acad Sci USA 1988;85:6617–21.
[12] Heppner FL, Musahl C, Arrighi I, Klein MA, Rulicke T, Oesch B, et al. Prevention of scrapie pathogenesis by transgenic expression of anti-prion protein antibodies. Science 2001;294:178–82.
[13] White AR, Enever P, Tayebi M, Mushens R, Linehan J, Brandner S, et al. Monoclonal antibodies inhibit prion replication and delay the development of prion disease. Nature 2003;422:80–3.
[14] Nashar TO, Amin T, Marcello A, Hirst TR. Current progress in the development of the B subunits of cholera toxin and *Escherichia coli* heat-labile enterotoxin as carriers for the oral delivery of heterologous antigens and epitopes. Vaccine 1993;11:235–40.
[15] Holmgren J, Czerkinsky C, Eriksson K, Mharandi A. Mucosal immunisation and adjuvants: a brief overview of recent advances and challenges. Vaccine 2003;21(Suppl. 2):S89–95.
[16] Tsuji T, Yokochi T, Kamiya H, Kawamoto Y, Miyama A, Asano Y. Relationship between a low toxicity of the mutant A subunit of enterotoxigenic *Escherichia coli* enterotoxin and its strong adjuvant action. Immunology 1997;90:176–82.
[17] Hornemann S, Glockshuber R. Autonomous and reversible folding of a soluble amino-terminally truncated segment of the mouse prion protein. J Mol Biol 1996;261:614–9.
[18] Peretz D, Williamson RA, Kaneko K, Vergara J, Leclerc E, Schmitt-Ulms G, et al. Antibodies inhibit prion propagation and clear cell cultures of prion infectivity. Nature 2001;412:739–43.
[19] Nicotera P. A route for prion neuroinvasion. Neuron 2001;31:345–8.
[20] Ghosh S. Intestinal entry of prions. Z Gastroenterol 2002;40:37–9.
[21] Wilesmith JW, Wells GA, Cranwell MP, Ryan JB. Bovine spongiform encephalopathy: epidemiological studies. Vet Rec 1988;123:638–44.
[22] Llewelyn CA, Hewitt PE, Knight RSG, Amar K, Cousens S, Mackenzie J, et al. Possible transmission of variant Creutzfeldt-Jakob disease by blood transfusion. Lancet 2004;363:417–21.
[23] Peden AH, Head MW, Ritchie DL, Bell JE, Ironside JW. Preclinical vCJD after blood transfusion in a PRNP codon 129 heterozygous patient. Lancet 2004;364:527–9.
[24] Goni F, Knudsen E, Schreiber F, Scholtzova H, Pankiewicz J, Carp R, et al. Mucosal vaccination delays or prevents prion infection via an oral route. Neuroscience 2005;133:413–21.
[25] Behar SM, Porcelli SA. Mechanisms of autoimmune disease induction. The role of the immune response to microbial pathogens. Arthritis Rheum 1995;38:458–76.
[26] Ang CW, Jacobs BC, Laman JD. The Guillain-Barre syndrome: a true case of molecular mimicry. Trends Immunol 2004;25:61–6.
[27] Koller MF, Grau T, Christen P. Induction of antibodies against murine full-length prion protein in wild-type mice. J Neuroimmunol 2002;132:113–6.
[28] Rosset MB, Ballerini C, Gregoire S, Metharom P, Carnaud C, Aucouturier P. Breaking immune tolerance to the prion protein using prion

protein peptides plus oligodeoxynucleotide-CpG in mice. J Immunol 2004;172:5168–74.
[29] Gilch S, Wopfner F, Renner-Muller I, Kremmer E, Bauer C, Wolf E, et al. Polyclonal anti-PrP auto-antibodies induced with dimeric PrP interfere efficiently with PrPSc propagation in prion-infected cells. J Biol Chem 2003;278:18524–31.
[30] Nikles D, Bach P, Boller K, Merten CA, Montrasio F, Heppner FL, et al. Circumventing tolerance to the prion protein (PrP): vaccination with PrP-displaying retrovirus particles induces humoral immune responses against the native form of cellular PrP. J Virol 2005;79:4033–42.

Available online at www.sciencedirect.com
ScienceDirect
Bioorganic & Medicinal Chemistry Letters
ELSEVIER
Bioorganic & Medicinal Chemistry Letters 16 (2006) 5982–5987

Metal complexes with superoxide dismutase-like activity as candidates for anti-prion drug

Tomoko Fukuuchi,[a,b,*] Katsumi Doh-ura,[c] Shin'ichi Yoshihara[b] and Shigeru Ohta[a]

[a]*Graduate School of Biomedical Sciences, Hiroshima University, 1-2-3 Kasumi, Minami-ku, Hiroshima 734-8553, Japan*
[b]*Faculty of Pharmaceutical Sciences, Hiroshima International University, 5-1-1 Koshingai, Hiro, Kure, Hiroshima 737-0112, Japan*
[c]*Graduate School of Medicine, Tohoku University, 2-1 Seiryo-cho, Aoba-ku, Sendai 980-8575, Japan*

Received 28 July 2006; revised 29 August 2006; accepted 30 August 2006
Available online 20 September 2006

Abstract—Various compounds were evaluated for ability to inhibit the formation of the abnormal protease-resistant form of prion protein (PrP-res) in two cell lines infected with different prion strains. Examination of the structure–activity relationships indicated that compounds with copper-selective chelating ability and whose copper complexes have high SOD-like activity are candidates for anti-prion drug.

Transmissible spongiform encephalophathies (TSEs) or prion diseases are a group of fatal neurodegenerative disorders, and their development is associated with accumulation of aggregated proteins, oxidative damage to the brain, and neuronal cell loss. Prion diseases are characterized by the generation of a protein molecule termed PrP^{Sc} (scrapie isoform of the prion protein), which is a conformational variant of the normal host protein, PrP^{C} (cellular isoform of the prion protein).[1,2] It is believed that the conversion of PrP^{C} into PrP^{Sc} is the key event in the pathogenesis of TSEs.

The octapeptide repeat region of the PrP^{C} binds several copper ions with concentration of the micromolar range[3,4] and their dissociation constant for the ion is reported to be femtomolar range.[5] The biological significance of this interaction is not clear, but it is reported that PrP^{C} has a copper-dependent superoxide dismutase (SOD) activity[6] and PrP^{C} may be involved in copper uptake into cells.[7,8] Recently, there has been increasing interest in the role of metal ions, in particular copper, in prion diseases.[9,10]

In the early 1970s, it was reported that the copper chelator cuprizone induced prion diseases-like histopathological changes in mice.[11,12] On the other hand, Sigurdsson et al. recently found that a copper chelator, D-penicillamine, delayed the onset of prion disease in infected mice, and suggested that chelator-based therapy might attenuate the disease.[13] Copper has been implicated in the pathogenesis of prion disease, but numerous studies have only succeeded in demonstrating the complexity of the effects of copper on the development of prion diseases, and it remains unclear whether this ion promotes or inhibits disease progression.

In the present study, we evaluated the ability of a wide range of compounds[14] to inhibit the formation of the abnormal protease-resistant form of prion protein (PrP-res), using two cell lines, ScN2a cells and F3, infected with different prion strains.[15,16] We then analyzed the structure–activity relationships to investigate what kinds of structure or biochemical characteristics contribute to anti-prion activity.

Spectrophotometric complexation studies.[17–19] The complexes were prepared as previously reported.[20,21] Solutions of 10 mM $Cu(ClO_4)_2$ and 8-hydroxyquinoline were prepared in H_2O. Cu(II)-chelate formation of 8-hydroxyquinoline was demonstrated by Job's method.[18,19] The spectrophotometric complexation studies showed that 8-hydroxyquinoline binds in 2:1 ratio with Cu(II) (Fig. 1A). 2,2′-Biquinoline, neocuproine, bathocuproine, 4,4′-dicarboxy-2,2′-biquinoline, porphyrins, cimetidine and D-penicillamine bind in 1:1 ratio with Cu(II) (2,2′-biquinoline, Fig. 1B; others, data not

Keywords: Prion; 2,2′-Biquinoline; Cimetidine; TPEN; Copper; Chelate; Metal complex; SOD activity.
* Corresponding author. Tel./fax: +81 823 73 8573; e-mail: t-fukuu@ps.hirokoku-u.ac.jp

0960-894X/$ - see front matter © 2006 Elsevier Ltd. All rights reserved.
doi:10.1016/j.bmcl.2006.08.115

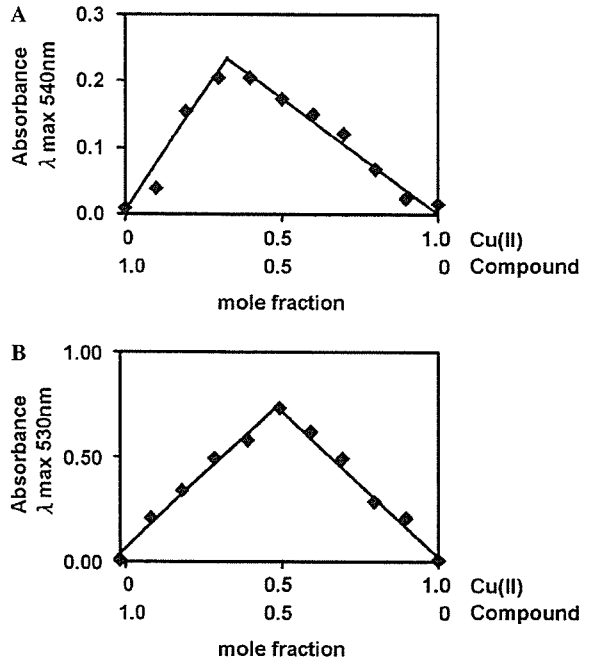

Figure 1. Continuous variation plots for 8-hydroxyquinoline and Cu(II) (A) and 2,2′-biquinoline and Cu(II) (B). (A) 2:1 binding ratio between 8-hydroxyquinoline and Cu(II), (B) 1:1 binding ratio between 2,2′-biquinoline and Cu(II). The plots were obtained by Job's method in aqueous solution.

shown). However, it has been reported that the oxidation state of copper may be altered in the D-penicillamine complex, and the complex prepared in this way contains both Cu(I) and Cu(II).[22]

Inhibition of PrP-res formation in ScN2a cells and F3 cells by metal chelators.[23–26] 1,10-Phenanthroline, 2,2′,2″-terpyridine and 8-hydroxyquinoline did not inhibit PrP-res formation within a nontoxic dose range (Table 1), but were cytotoxic at 100 nM. Chelators of this class can chelate a wide variety of metals.

Neocuproine, bathocuproine, 2,2′-biquinoline and 4,4′-dicarboxy-2,2′-biquinoline are highly specific copper chelators. The chelators of this class, except 4,4′-dicarboxy-2,2′-biquinoline, effectively inhibited PrP-res formation in ScN2a cells and F3 cells in a dose-dependent manner (Fig. 2). The concentrations giving 50% inhibition (IC_{50}) of PrP-res formation in ScN2a cells relative to the DMSO-treated or untreated control ranged from 5 to 80 nM (Table 1). These compounds showed no apparent cytotoxicity at concentrations up to 1 μM. However, neocuproine was ineffective in F3 cells within a nontoxic dose range. Findings from these experiments suggest that compounds having copper-selective chelating ability are more effective inhibitors than non-selective metal-chelating compounds, but not an exclusive factor.

Inhibition of PrP-res formation in ScN2a cells and F3 cells by porphyrins.[23–26] Porphyrins can form 1:1 stable chelates with various metal ions. The order of stability for divalent metal ions is Cu > Fe > Zn > Mn, regardless of the type of substituents on the porphyrin ring. Porphyrins were effective inhibitors of PrP-res formation, with IC_{50} values ranging from 5 to 320 nM in ScN2a cells and F3 cells (Table 2). And Mn(III)–porphyrins complexes showed higher anti-prion activity than the metal-free compounds (Table 2).

SOD-like activity and correlation with anti-prion activity. It is known that Mn(III)–porphyrin complexes show high SOD-like activity in vitro and in vivo.[27,28] We thought that SOD-like activity might contribute to the anti-prion activity of such compounds, since the SOD activity of PrP^C is decreased by conversion to PrP^{Sc}. Therefore, we focused on chelators having SOD-like activity. Many low-molecular metal complexes, mainly copper, manganese and iron complexes, have been synthesized and their SOD-like activity examined in vitro and in vivo,[29–33] and some of them showed activity in vivo.[34–36] As shown in Table 3, SOD-like activity of these compounds was measured in vitro by our methods.[37] The SOD-like activity in cell lysates was significantly increased when these metal-free compounds were added to the cell cultures (data not shown). Therefore, the chelators that showed anti-prion activity formed metal complexes and had SOD-like activity.

Among these compounds, we chose cimetidine[34,38] and TPEN[39] for further examination, as well as Mn-TCPP (Mn-TBAP), which we had already examined. Cimetidine effectively inhibited PrP-res formation, with IC_{50} values of 5 nM in ScN2a cells and 200 nM in F3 cells. TPEN inhibited PrP-res formation, with IC_{50} values of 5 nM in ScN2a cells and 200 nM in F3 cells.

We found that the compounds, shown in Tables 1 and 2, with higher anti-prion activity in ScN2a cells had higher SOD-like activity (Table 3). Statistical analysis exhibited a significant linear correlation between these two activities ($r = 0.93$) (Fig. 3).

Despite numerous studies, it remains unclear whether copper ions promote[13] or inhibit[40] prion disease. In Alzheimer's disease, another neurodegenerative disease, the copper- and zinc-selective chelator clioquinol was effective in decreasing β-amyloid deposits.[41] However, Doh-ura et al. found that clioquinol and related compounds, quinoline hydrochloride, 8-hydroxyquinoline, and 8-acetoxyquinoline, were ineffective in scrapie-infected mouse neuroblastoma (ScNB) cells.[25] Thus, chelating drugs that are effective in inhibiting β-amyloid formation may not inhibit the conversion of PrP^C to PrP^{Sc}.

In this study, we evaluated the anti-prion activity of various compounds having metal-chelating ability in order to identify the requirements for anti-prion activity. We found that many, but not all, compounds having selective copper-chelating ability are effective inhibitors of PrP-res formation in ScN2a cells and F3 cells. Thus, copper-selective chelating ability per se may not be essential for anti-prion activity. This idea is supported by the observation that porphyrins chelating manganese

Table 1. Inhibition of PrP-res formation in ScN2a cells and F3 cells by metal chelators

Compound	Structure	Metal(M)	Inhibition PrP-res IC_{50} (nM)	
			ScN2a cells	F3 cells
1,10-Phenanthroline	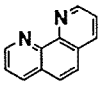		N.E.	N.E.
2,2′,2″-Terpyridine	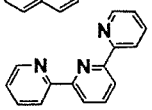		N.E.	N.E.
8-Hydroxyquinoline			N.E.	N.E.
Bis(8-quinolinolato) Copper(II)		Cu^{2+}	N.E.	N.E.
Bis(8-quinolinolato) Zinc(II)		Zn^{2+}	N.E.	N.E.
Neocuproine	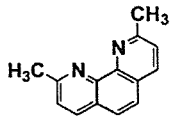		80	N.E.
Bathocuproine	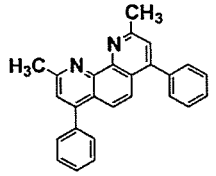		80	200
2,2′-Biquinoline	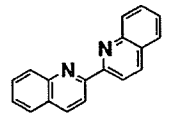		5	250
4,4′-Dicarboxy-2,2′-biquinoline	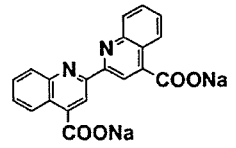		N.E.	N.E.

N.E., no effect.
IC_{50}, concentration of a compound causing 50% inhibition of PrP-res formation relative to the control.

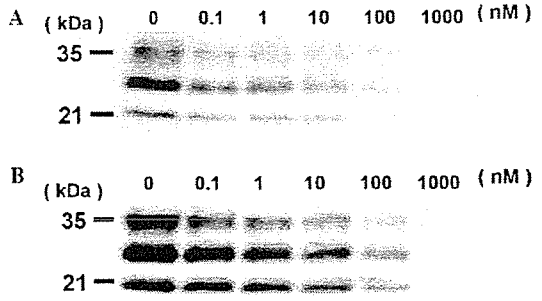

Figure 2. Anti-prion activity of 2,2′-biquinoline in prion-infected cells. Various concentrations of the compound were added to freshly passaged ScN2a cells (A) or F3 cells (B), and the PrP-res levels were analyzed by Western blotting. Lanes: 0, cells treated with DMSO alone; others, treated with the indicated concentration of 2,2′-biquinoline. Bars on the left indicate molecular mass markers at 35 and 21 kDa.

showed greater anti-prion activity than the metal-free compounds. Therefore, we examined whether SOD-like activity was associated with anti-prion activity, and discovered that this was the case.

PrP^C plays an important role in cell protection from oxidative stress, and modulates the activity of antioxidant enzymes by regulating the intracellular copper concentration, but it can also play a direct role owing to its intrinsic SOD activity.[6,42,43] Cells with accumulated abnormal PrP^{Sc} displayed the phenotypes of decreased copper-binding capacity and higher sensitivity to oxidative stress.[16,44] Interestingly, we found a significant correlation ($r = 0.93$) between SOD-like activity and anti-prion activity. Furthermore, we confirmed that the copper complex of D-penicillamine, which has been reported

Table 2. Inhibition of PrP-res formation in ScN2a cells and F3 cells by porphyrins

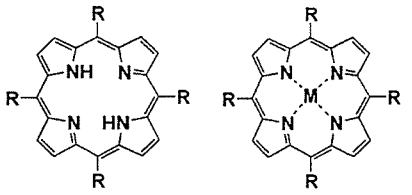

Compound	R	Metal(M)	Inhibition PrP-res IC_{50} (nM)	
			ScN2a cells	F3 cells
TPP			10	320
TCPP	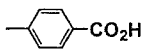		250	160
Mn-TCPP (MnTBAP)	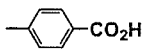	Mn^{3+}	40	60
TPPS	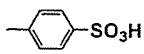		200	160
TMPyP	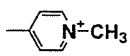		130	160
Mn-TMPyP	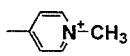	Mn^{3+}	5	40

IC_{50}, concentration of a compound giving 50% inhibition of PrP-res formation relative to the control.

Table 3. SOD-like activity of metal complexes

Chelating metal	Compound	SOD-like activity IC_{50} (μM)
Cu	8-Hydroxyquinoline	263
	Clioquinol	140
	Neocuproine	50
	Bathocuproine	32
	2,2′-Biquinoline	3
	4,4′-Dicarboxy-2,2′-biquinoline	263
	Cimetidine	0.4
	D-Penicillamine	28
Mn	TCPP	8
	TMPyP	0.3
Fe	TPEN	0.4

IC_{50}, concentration of a compound giving 50% inhibition of WST-1 reduction.

to show anti-prion activity, exhibits SOD-like activity.[13]

It is not easy to find molecules with both good metal-binding ability and high SOD-like activity, because, taking copper ions as an example, the former property means the Cu(II) complex is rather stable, while the latter property implies that the complex is prone to be reduced to the Cu(I)-chelator state.[45] This might explain why compounds such as clioquinol that are good copper chelators are nevertheless ineffective in terms of anti-prion activity.[25]

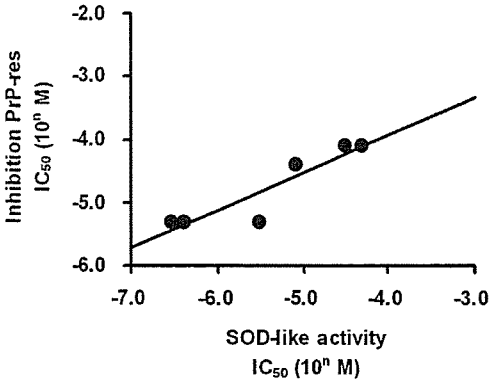

Figure 3. Correlation between SOD-like activity and inhibition of PrP-res formation in ScN2a cells. The plot shows data from seven compounds for which both SOD activity and inhibition of PrP-res formation were determined. ($r = 0.93$) SOD-like activity IC_{50}: concentration of a compound giving 50% inhibition of WST-1 reduction. Inhibition PrP-res IC_{50}: concentration of a compound giving 50% inhibition of PrP-res formation relative to the control.

On the other hand, cimetidine can form complexes with both Cu(I) and Cu(II), and has satisfactory SOD-like activity in both states, so it may be a good candidate for anti-prion activity. Furthermore, cimetidine can cross the blood–brain barrier to act in the central nerve system.[46] This type of compounds may provide a possible therapeutic approach for prion diseases.

In conclusion, we suggest that compounds which have copper-selective chelating ability, and whose copper complexes have high SOD-like activity are candidates for anti-prion drug.

References and notes

1. Prusiner, S. B. *Science* **1982**, *216*, 136.
2. Bounias, M.; Purdey, M. *Sci. Total Environ.* **2002**, *297*, 1.
3. Brown, D. R.; Qin, K.; Herms, J. W.; Madlung, A.; Manson, J.; Strome, R.; Fraser, P. E.; Kruck, T.; von Bohlen, A.; Schulz-Schaeffer, W.; Giese, A.; Westaway, D.; Kretzschmar, H. *Nature* **1997**, *390*, 684.
4. Viles, J. H.; Cohen, F. E.; Prusiner, S. B.; Goodin, D. B.; Wright, P. E.; Dyson, H. J. *Proc. Natl. Acad. Sci. U.S.A.* **1999**, *96*, 2042.
5. Jackson, G. S.; Murray, I.; Hosszu, L. L.; Gibbs, N.; Waltho, J. P.; Clarke, A. R.; Collinge, J. *Proc. Natl. Acad. Sci. U.S.A.* **2001**, *98*, 8531.
6. Brown, D. R.; Wong, B. S.; Hafiz, F.; Clive, C.; Haswell, S. J.; Jones, I. M. *Biochem. J.* **1999**, *344*, 1.
7. Brown, D. R. *J. Neurosci. Res.* **1999**, *58*, 717.
8. Pauly, P. C.; Harris, D. A. *J. Biol. Chem.* **1998**, *273*, 33107.

9. McKenzie, D.; Bartz, J.; Mirwald, J.; Olander, D.; Marsh, R.; Aiken, J. *J. Biol. Chem.* **1998**, *273*, 25545.
10. Brown, D. R.; Hafiz, F.; Glass-smith, L. L.; Wong, B. S.; Jones, I. M.; Clive, C.; Haswell, S. J. *EMBO J.* **2000**, *19*, 1180.
11. Kimberlin, R. H.; Millson, G. C.; Bountiff, L.; Collis, S. C. *J. Comp. Pathol.* **1974**, *84*, 263.
12. Pattison, I. H.; Jebbett, J. N. *Nature* **1971**, *230*, 115.
13. Sigurdsson, E. M.; Brown, D. R.; Alim, M. A.; Scholtzova, H.; Carp, R.; Meeker, H. C.; Prelli, F.; Frangione, B.; Wisniewski, T. *J. Biol. Chem.* **2003**, *278*, 46199.
14. Copper(II) perchlorate hexahydrate 98% and D-penicillamine were purchased from Sigma. Iron(II) sulfate heptahydrate, 2,2′-biquinoline, and cimetidine were purchased from Wako Pure Chemical (Osaka, Japan). 1,10-Phenanthroline monohydrate, 2,9-dimethyl-4,7-dimethyl-1,10-phenanthroline (bathocuproine), 2,9-1,10-phenanthroline (neocuproine), tetraphenylporphine (TPP), tetraphenylporphine tetrasulfonic acid (TPPS), α,β,γ,δ-tetrakis(1-methylpyridinium-4-yl)porphine *p*-toluenesulfonate (TMPyP), tetrakis(4-carboxyphenyl)porphine (TCPP), 2,2′-bicinchoninic acid dipotassium salt, 5-chloro-7-iodo-8-hydroxyquinoline (clioquinol), and 8-hydroxyquinoline were purchased from Tokyo Kasei (Tokyo, Japan). Manganese(III) tetrakis(1-methylpyridinium-4-yl)porphyrin pentachloride (Mn-TMPyP) and Mn(III)tetrakis(4-benzoic acid)porphyrin chloride(Mn-TCPP or Mn-TBAP) were purchased from Calbiochem (California, USA). They were dissolved in 100% dimethylsulfoxide (DMSO) or 95% ethanol just before use.
15. Two types of prion-infected mouse neuroblastoma (N2a) cell lines were used in this study: N2a cells infected with the RML strain (ScN2a) [16] and N2a#58 cells infected with the Fukuoka-1 strain (F3). N2a#58 cells are known to express five times more normal PrP than N2a cells. Both ScN2a cells and F3 cells were grown in six-well culture plates in Opti-MEM (Invitrogen) supplemented with 10% fetal bovine serum. The cells were allowed to reach confluence, and chemicals at various concentrations were added to the medium when 5% of the confluent cells were passaged.The final concentration of either DMSO or ethanol in the medium was less than 0.2%. The cultures were allowed to grow to confluence (3 or 4 days).
16. Milhavet, O.; McMahon, H. E.; Rachidi, W.; Nishida, N.; Katamine, S.; Mange, A.; Arlotto, M.; Casanova, D.; Riondel, J.; Favier, A.; Lehmann, S. *Proc. Natl. Acad. Sci. U.S.A.* **2000**, *97*, 13937.
17. The chelation study was carried out using Job's method.[18,19] Solutions of 10 mM Cu(II) and each compound at a compound:Cu (II) ratio of 1:0 to 0:1 were prepared in ultrapure water (MilliQ; Millipore Co., Japan) or 95% ethanol, and λmax of the copper complex was measured.
18. Vosburgh, W. C.; Cooper, G. R. *J. Am. Chem. Soc.* **1941**, *63*, 437.
19. Job, P. *Ann. Chim.* **1928**, *9*, 113.
20. Kolthoff, I. M. S.; Sandell, E. B. *Textbook of Quantitative Inorganic Analysis*; Pergamon Press: New York, 1959, The MacMillan Co.
21. Ueno, K.; Imamura, T.; Cheng, K. L. *Handbook of Organic Analytical Reagents*; Pergamon Press: Tokyo, 1992, CRC Press.
22. Birker, P. J.; Freeman, H. C. *J. Am. Chem. Soc.* **1977**, *99*, 6890.
23. The anti-prion activity of each compound was assayed by measuring the 50%-inhibitory concentration (IC_{50}) for PrP-res formation in ScN2a cells and F3 cells, as described in previous reports.[24–26] Briefly, compounds were added at designated concentrations to the medium when cells were passaged at 10% confluency. The cells were allowed to grow to confluence and lysed with lysis buffer (0.5% sodium deoxycholate, 0.5% Nonidet P-40, and PBS). The lysates were digested with 10 μg/ml proteinase K for 30 min at 37 °C and centrifuged at 15,000 rpm for 5 min at 24 °C with GLASSFOG(Q-bio gene, USA). The pellets were resuspended in sample loading buffer and boiled. Samples were separated by electrophoresis on 15% Tris–glycine–SDS–polyacrylamide gel and electroblotted. PrP-res was detected using an antibody, SAF83 (1:5000; SPI-Bio, France), followed by an alkaline phosphatase-conjugated secondary antibody. Immunoreactive signals were visualized using CDP-Star detection reagent (Amersham Biosciences Corp., U.S.A.) and were analyzed densitometrically. At least three independent experiments were performed to estimate IC_{50} of each compound.
24. Doh-Ura, K.; Iwaki, T.; Caughey, B. *J. Virol.* **2000**, *74*, 4894.
25. Murakami-Kubo, I.; Doh-ura, K.; Ishikawa, K.; Kawatake, S.; Sasaki, K.; Kira, J.; Ohta, S.; Iwaki, T. *J. Virol.* **2004**, *78*, 1281.
26. Ishikawa, K.; Doh-ura, K.; Kudo, Y.; Nishida, N.; Murakami-Kubo, I.; Ando, Y.; Sawada, T.; Iwaki, T. *J. Gen. Virol.* **2004**, *85*, 1785.
27. Day, B. J.; Shawen, S.; Liochev, S. I.; Crapo, J. D. *J. Pharmacol. Exp. Ther.* **1995**, *275*, 1227.
28. Day, B. J.; Crapo, J. D. *Toxicol. Appl. Pharmacol.* **1996**, *140*, 94.
29. Younes, M.; Lengfelder, E.; Zienau, S.; Weser, U. *Biochem. Biophys. Res. Commun.* **1978**, *81*, 576.
30. Kimura, E.; Sakonaka, A.; Nakamoto, M. *Biochim. Biophys. Acta* **1981**, *678*, 172.
31. Kimura, E.; Yatsunami, A.; Watanabe, A.; Machida, R.; Koike, T.; Fujioka, H.; Kuramoto, Y.; Sumomogi, M.; Kunimitsu, K.; Yamashita, A. *Biochim. Biophys. Acta* **1983**, *745*, 37.
32. Wada, K.; Fujibayashi, Y.; Yokoyama, A. *Arch. Biochem. Biophys.* **1994**, *310*, 1.
33. Goldstein, S.; Czapski, G. *Free Radic. Res. Commun.* **1991**, *12–13*, 205.
34. Baudry, M.; Etienne, S.; Bruce, A.; Palucki, M.; Jacobsen, E.; Malfroy, B. *Biochem. Biophys. Res. Commun.* **1993**, *192*, 964.
35. Darr, D. J.; Yanni, S.; Pinnell, S. R. *Free Radic. Biol. Med.* **1988**, *4*, 357.
36. Wada, K.; Fujibayashi, Y.; Tajima, N.; Yokoyama, A. *Biol. Pharm. Bull.* **1994**, *17*, 701.
37. SOD-like assay kit-WST (Dojindo Chemical, Kumamoto, Japan) was used for the quantification of SOD-like activity. This method is a xanthine-based spectrophotometric assay using the tetrazolium salt WST-1. The SOD-like activity was evaluated using the standard curve of SOD-like activity versus absorbance at 450 nm. Differences of SOD-like activity were tested by use of the unpaired Student's *t* test, and *p* values smaller than 0.05 were considered to be statistically significant.
38. Kimura, E.; Koike, T.; Shimizu, Y.; Kodama, M. *Inorg. Chem.* **1986**, *25*, 2242.
39. Nagano, T.; Hirano, T.; Hirobe, M. *J. Biol. Chem.* **1989**, *264*, 9243.
40. Hijazi, N.; Shaked, Y.; Rosenmann, H.; Ben-Hur, T.; Gabizon, R. *Brain Res.* **2003**, *993*, 192.
41. Cherny, R. A.; Atwood, C. S.; Xilinas, M. E.; Gray, D. N.; Jones, W. D.; McLean, C. A.; Barnham, K. J.; Volitakis, I.; Fraser, F. W.; Kim, Y.; Huang, X.; Goldstein, L. E.; Moir, R. D.; Lim, J. T.; Beyreuther, K.;

Zheng, H.; Tanzi, R. E.; Masters, C. L.; Bush, A. I. *Neuron* **2001**, *30*, 665.
42. Martins, V. R.; Mercadante, A. F.; Cabral, A. L.; Freitas, A. R.; Castro, R. M. *Braz. J. Med. Biol. Res.* **2001**, *34*, 585.
43. Rachidi, W.; Vilette, D.; Guiraud, P.; Arlotto, M.; Riondel, J.; Laude, H.; Lehmann, S.; Favier, A. *J. Biol. Chem.* **2003**, *278*, 9064.
44. Rachidi, W.; Mange, A.; Senator, A.; Guiraud, P.; Riondel, J.; Benboubetra, M.; Favier, A.; Lehmann, S. *J. Biol. Chem.* **2003**, *278*, 14595.
45. Li, Q. X.; Luo, Q. H.; Li, Y. Z.; Shen, M. C. *Dalton Trans.* **2004**, 2329.
46. Totte, J.; Scharpe, S.; Verkerk, R.; Neels, H.; Vanhaeverbeek, M.; Smitz, S.; Rousseau, J. J. *Lancet* **1981**, *1*, 1047.

Journal of Neurochemistry, 2006, **99**, 198–205 doi:10.1111/j.1471-4159.2006.04035.x

Styrylbenzoazole derivatives for imaging of prion plaques and treatment of transmissible spongiform encephalopathies

Kensuke Ishikawa,* Yukitsuka Kudo,† Noriyuki Nishida,‡ Takahiro Suemoto,§ Tohru Sawada,§ Toru Iwaki¶ and Katsumi Doh-ura*

**Department of Prion Research, Tohoku University Graduate School of Medicine, Sendai, Japan*

†Division of Telecommunication and Information Technology, Biomedical Engineering Research Organization, Tohoku University, Sendai, Japan

‡Division of Cellular and Molecular Biology, Nagasaki University Graduate School of Biomedical Sciences, Nagasaki, Japan

§BF Research Institute Inc., Osaka, Japan

¶Department of Neuropathology, Graduate School of Medical Sciences, Kyushu University, Fukuoka, Japan

Abstract

Recent prevalence of acquired forms of transmissible spongiform encephalopathies (TSEs) has urged the development of early diagnostic measures as well as therapeutic interventions. To extend our previous findings on the value of amyloid imaging probes for these purposes, styrylbenzoazole derivatives with better permeability of blood–brain barrier (BBB) were developed and analyzed in this study. The new styrylbenzoazole compounds clearly labeled prion protein (PrP) plaques in brain specimens from human TSE in a manner irrespective of pathogen strain, and a representative compound BF-168 detected abnormal PrP aggregates in the brain of TSE-infected mice when the probe was injected intravenously. On the other hand, most of the compounds inhibited abnormal PrP formation in TSE-infected cells with IC_{50} values in the nanomolar range, indicating that they represent one of the most potent classes of inhibitor ever reported. BF-168 prolonged the lives of mice infected intracerebrally with TSE when the compound was given intravenously at the preclinical stage. The new compounds, however, failed to detect synaptic PrP deposition and to show pathogen-independent therapeutic efficacy, similar to the amyloid imaging probes we previously reported. The compounds were BBB permeable and non-toxic at doses for imaging and treatment; therefore, they are expected to be of practical use in human TSE.

Keywords: amyloid imaging, anti-prion activity, pathogen strain, prion disease, styrylbenzoazole derivatives.

J. Neurochem. (2006) **99**, 198–205.

The transmissible spongiform encephalopathies (TSEs) or prion diseases form a group of neurodegenerative disorders characterized by abnormal deposition of protease-resistant isoforms of prion protein (PrP) in the CNS (Prusiner 1991). TSEs are classified as sporadic, hereditary or environmentally acquired, and have become a serious public health issue because of the recent prevalence of acquired Creutzfeldt–Jakob disease (CJD), such as the variant form due to bovine spongiform encephalopathy (Will *et al.* 1996) and the iatrogenic form with cadaveric growth hormone or dura grafts (Brown *et al.* 2000). There is an urgent need to develop prophylactic and therapeutic interventions as well as diagnostic measures at the preclinical or early clinical stages of these incurable diseases.

We have previously reported that some amyloid imaging compounds, primarily derived from amyloid dyes such as

Received February 16, 2006; revised manuscript received May 25, 2006; accepted May 30, 2006.

Address correspondence and reprint requests to Dr Kensuke Ishikawa, Division of Prion Biology, Department of Prion Research, Tohoku University Graduate School of Medicine, 2–1 Seiryo-machi, Aoba-ku, Sendai 980-8575, Japan. E-mail: ishikawa@mail.tains.tohoku.ac.jp

Abbreviations used: AD, Alzheimer's disease; BBB, blood–brain barrier; BSB, (trans, trans)-1-bromo-2,5-bis-(3-hydroxycarbonyl-4-hydroxy)styrylbenzene; CJD, Creutzfeldt–Jakob disease; DMSO, dimethylsulfoxide; FDDNP, 2-(1-[6-[(2-fluoroethyl)(methyl)amino]-2-naphthyl]ethylidene)malononitrile; GSS, Gerstmann–Sträussler–Scheinker syndrome; ICR, Institute of Cancer Research; ID, injected dose; NT, not tested; PrP, prion protein; PrPres, protease-resistant PrP; PTA, phosphotungstic acid; PVDF, polyvinylidene difluoride; TSE, transmissible spongiform encephalopathy.

Congo red and thioflavin T, are useful for detection of prion plaques and treatment of TSE (Ishikawa *et al.* 2004). These compounds, however, are limited in their ability because of inefficient brain uptake. Here we describe new compounds, styrylbenzoazole derivatives, which have been developed for practical use and analyzed for their PrP imaging ability, anti-prion activity, therapeutic efficacy, brain uptake and toxicity.

Materials and methods

Chemicals and experimental models

All of the test compounds were synthesized at Tanabe R & D (Saitama, Japan) and used freshly after being dissolved in 100% dimethylsulfoxide (DMSO).

Cultured cells were grown in Opti-MEM (Invitrogen, Carlsbad, CA, USA) supplemented with 10% fetal calf serum. As cellular models of TSE, we used mouse neuroblastoma (N2a) cells persistently infected with the RML strain (ScN2a) (Race *et al.* 1988) and six other prion-infected cell lines: N2a58 cells individually infected with the RML strain, the 22L strain (Nishida *et al.* 2000) and Fukuoka-1 strain (Ishikawa *et al.* 2004); N2a cells infected with the 22L strain; mouse hypothalamic cells (GT1-7) infected with the 22L strain (Milhavet *et al.* 2000); and mouse fibroblast cells (L929) infected with the RML strain (Vorberg *et al.* 2004).

Tg7 mice overexpressing hamster PrP (Race *et al.* 1995) and Tga20 mice overexpressing mouse PrP (Fischer *et al.* 1996) were also used. These mouse models were intracerebrally infected with 20 μL brain homogenate comprising 1% (w/v) of the 263K strain and the RML strain respectively. The Tg7 mice showed plaque-type PrP deposition between the cerebral cortex and hippocampus by 6 weeks after infection, followed by synaptic-type PrP deposition in the thalamus. The Tga20 mice showed similar pathological deposition, but plaques were not seen as frequently. Each mouse weighed ~30 g, and was maintained under deep ether anesthesia for minimum distress during all surgical procedures. Permission for the animal study was obtained from either the Animal Experiment Committee of Kyushu University or Tohoku University, Japan.

Brain uptake study

Test compounds were administered intravenously to Institute of Cancer Research (ICR) mice under ether anesthesia to determine initial brain uptakes. At 2 or 30 min after injection, the brains were removed, weighed and homogenized with saline. After centrifugation of the homogenate at 21 900 *g* for 10 min, the supernatant was applied to a conditioned C18 solid-phase extraction cartridge, and the compounds were eluted with methyl alcohol. Fluorescence was detected by high performance liquid chromatography with a fluorescence detector as reported previously (Okamura *et al.* 2005), and the percentage of injected dose per gram (%ID/g) was used as a measure of the level of the compounds in the brain.

In vitro PrP imaging in sections

Autopsy-diagnosed brain samples from cases of Gerstmann–Sträussler–Scheinker syndrome (GSS) ($n = 2$), sporadic CJD ($n = 5$), iatrogenic dura CJD with synaptic PrP deposition ($n = 1$) and non-TSE control cases with amyloid lesions [Alzheimer's disease (AD), $n = 2$] or without amyloid lesions (cerebral infarction, $n = 1$) were obtained from the Department of Neuropathology, Kyushu University, Japan. After fixation in 10% buffered formalin for 2 weeks, each sample of TSE was immersed in 98% formic acid for the reduction of prion infectivity, embedded in paraffin and cut into sections 7 μm thick. Sections of a variant CJD case were kindly provided by Dr James W. Ironside of the CJD Surveillance Unit, Edinburgh, UK. For neuropathological staining, deparaffinized sections were immersed in 1% Sudan black solution to quench tissue autofluorescence. They were then incubated for 30 min in 1-μM solutions of the test compounds, rinsed with distilled water and examined under a fluorescence microscope (DMRXA; Leica Instruments, Wetzler, Germany) with a UV or FITC filter set.

For comparison, each section was subsequently immunoassayed for PrP as described previously (Doh-ura *et al.* 2000). Briefly, the sections were treated with a hydrolytic autoclave and incubated with a rabbit primary antibody, c-PrP, which was raised against a mouse PrP fragment, amino acids 214–228 (1 : 200; Immuno-Biological Laboratories, Gunma, Japan), followed by incubation with a horseradish peroxidase-conjugated secondary antibody (1 : 200; Vector Laboratories, Burlingame, CA, USA). The reaction product was developed with 3,3′-diaminobenzidine tetrahydrochloride solution and counterstained with hematoxylin. Paraffin-embedded brains of experimental animals were similarly investigated.

In vivo PrP imaging in model animals

BF-168 (molecular weight 312.34) dissolved in 10% DMSO was administered intravenously (0.5–5 mg/kg body weight) into Tg7 mice at 6–7 weeks after injection when the mice showed no apparent clinical signs of TSE. As controls, vehicle alone was similarly injected into infected mice, and BF-168 was administered into uninfected mice. The animals were killed at various time points, and the brains were rapidly frozen and cut into coronal sections 10 μm thick using a cryostat (CM3050; Leica Instruments). The sections were thaw-mounted on slides, dried and coverslipped. They were examined under a fluorescence microscope and further analyzed immunohistochemically as described above.

In vitro treatment in cell cultures

Abnormal PrP formation was assayed by the content of protease-resistant PrP (PrPres) in cellular models of TSE as described previously (Caughey and Raymond 1993). Each compound was added at the designated concentrations when cells were passaged at 10% confluence, while maintaining the final concentration of DMSO in the medium at < 0.5%. The cells were allowed to grow to confluence and lysed with lysis buffer (0.5% sodium deoxycholate, 0.5% Nonidet P-40, phosphate-buffered saline). For analysis of PrPres, samples were digested with 10 μg/mL proteinase K for 30 min, and the digestion was stopped with 0.5 mM phenylmethylsulfonyl fluoride. The samples were centrifuged at 100 000 *g* for 30 min, and pellets were resuspended in 1 × sample loading buffer and boiled. For analysis of cellular PrP in N2a cells, cell lysates were mixed directly with a quarter volume of 5 × sample loading buffer and boiled. These samples were separated by electrophoresis on a 15% Tris–glycine–sodium dodecyl sulfate polyacrylamide gel and electroblotted on to a polyvinylidene difluoride (PVDF) filter (Millipore, Bedford, MA, USA). PrP was detected using a monoclonal antibody, SAF83 (1 : 5000; SPI-BIO, Massy, France), followed by an alkaline phosphatase-conjugated

goat anti-mouse antibody (1 : 20 000; Promega, Madison, WI, USA). Immunoreactive blots were visualized with CDP-Star detection reagent (Amersham, Piscataway, NJ, USA). More than two independent assays were performed in each experiment and signals were analyzed using image analysis software. The approximate concentration of the compound giving 50% inhibition of PrPres formation, relative to the vehicle-treated control (IC_{50}), was estimated by signal intensity. To control for the detection limits of western blotting, we performed additional experiments utilizing sodium phosphotungstic acid (PTA) precipitation, which is the most sensitive technique presently available to detect PrPres (Safar *et al.* 1998). The PTA precipitation was undertaken on cell lysates of ScN2a treated with BF-168 at a designated concentration. The resulting pellets were collected by centrifugation and then analyzed by immunoblotting as described above.

In vivo treatment in model animals

BF-168 solution (4 mg/kg body weight) or vehicle alone was injected intravenously to experimental animals ($n = 5$) once a week. The treatment was started at 2 weeks after injection for Tg7 mice and at 4 weeks after injection for Tga20 mice, and repeated for 4 weeks. A continuous subcutaneous infusion of BF-168 was also given to Tga20 mice ($n = 5$) using an Alzet osmotic pump (Durect, Cupertino, CA, USA). In accordance with the manufacturer's instructions, each pump was filled with BF-168 solution at the designated doses and placed in a subcutaneous area of the back at 4 weeks after injection. The animals showed no apparent adverse effects of the treatment and were monitored 5 days a week until obvious clinical signs appeared. Statistical significance was analyzed by one-way ANOVA followed by Scheffé's method for multiple comparisons.

Results

Brain uptake and toxicity

We designed and synthesized novel styrylbenzoxazole derivatives (Table 1), styrylbenzothiazole and styrylbenzoimidazole derivatives (Table 2) with more efficient permeability of the BBB and less toxicity. Values for brain uptake at 2 min after intravenous injection of the compounds were in the 2.4–17.0%ID/g range, indicating a satisfactory level for imaging probes. Their washouts from the brain varied, with the ratio of %ID/g at 2 min to that at 30 min after injection ranging from 1.0 to 56.9. Acute toxicity was tested by administering each compound intravenously at ~10 mg/kg body weight into normal ICR mice. No apparent toxic effect was observed with any of the compounds tested.

PrP imaging ability

Imaging of abnormal PrP deposition by the compounds was first performed in brain sections of human TSE. The compounds fluorescently labeled most of the PrP plaques in cerebellar cortices of both GSS cases (Fig. 1a, representative data). Among sections from the sporadic CJD cases, PrP deposition was labeled only in a case with plaques (Fig. 1c). In the cerebral cortex from the variant CJD case, large core plaques were detectable, whereas the majority of immunopositive aggregates were not labeled (Fig. 1e). In contrast, no fluorescence signal was identified in sections from the dura CJD case or the other sporadic CJD cases that

Table1 Chemical structure, PrPres inhibition and brain uptake of styrylbenzoxazole derivatives including BF-168

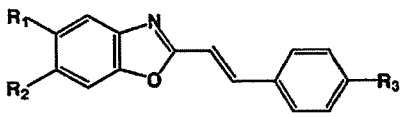

Compound	R_1	R_2	R_3	IC_{50} (nM)[a]	Brain uptake (%ID/g)[b] 2 min	Brain uptake (%ID/g)[b] 30 min	Ratio of 2 to 30 min brain uptake
BF-168	H	$O(CH_2)_2F$	$NH(CH_3)$	0.4	3.9[c]	1.6	2.4
BF-125	H	H	$N(C_2H_5)_2$	10.2	3.0	3.0	1.0
BF-133	F	H	$N(CH_3)_2$	1.6	5.5	3.8	1.4
BF-135	NO_2	H	$N(CH_3)_2$	< 1	NT[d]	NT	-
BF-140	F	H	NH2	< 1	5.5	1.1	5.0
BF-145	F	H	$NH(CH_3)$	< 1	4.4	1.6	2.8
BF-148	H	F	$N(CH_3)_2$	< 1	NT	NT	-
BF-165	H	H	$NH(CH_3)$	7.1	7.2	NT	-
BF-169	H	OH	$NH(CH_3)$	2.4	NT	NT	-
BF-173	I	H	NH_2	2.2	NT	NT	-
BF-180	I	H	$NH(CH_3)$	8.5	2.4	1.8	1.3
BF-191	H	H	Cl	1.8	12.0	1.7	7.1
BF-208	H	H	F	< 1	11.0	0.53	20.8
N-282	H	H	$N(CH_3)_2$	2.1	4.0	1.7	2.4
N-407	H	H	H	< 1	17.0	0.99	17.2

[a]IC_{50}, approximate concentration of a compound giving 50% inhibition of PrPres formation relative to the control in ScN2a cells.
[b]%ID/g, percentage of injected dose per gram in the brains of normal mice.
[c]already reported in the previous work (Okamura *et al.*, 2004).
[d]NT, not tested.

Table 2 Chemical structure, PrPres inhibition and brain uptake of styrylbenzothiazole and styrylbenzoimidazole derivatives

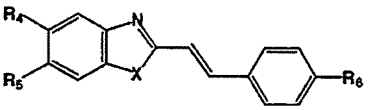

Compound	X	R_4	R_5	R_6	IC_{50} (nM)[a]	Brain uptake (%ID/g)[b] 2 min	Brain uptake (%ID/g)[b] 30 min	Ratio of 2 to 30min brain uptake
BF-124	S	H	H	$N(C_2H_5)_2$	18.1	2.4	2.5	1.0
BF-162	S	F	H	$N(CH_3)_2$	1.4	NT[c]	NT	-
N-276	S	H	H	$N(CH_3)_2$	< 1	NT	NT	-
N-438	S	H	H	H	< 1	11.0	2.0	5.5
BF-126	NH	H	H	$N(C_2H_5)_2$	21	7.2	0.16	45
BF-166	NH	F	H	$N(C_2H_5)_2$	1.1	NT	NT	-
N-457	NH	H	H	Cl	< 1	7.1	0.21	33.8
N-491	NH	H	H	H	1.9	7.4	0.13	56.9

[a]IC_{50}, approximate concentration of a compound giving 50% inhibition of PrPres formation relative to the control in ScN2a cells.
[b]%ID/g, percentage of injected dose per gram in the brains of normal mice.
[c]NT, not tested.

included perivacuolar and/or synaptic PrP deposition (data not shown). Background staining was barely observed after rinsing off the excess compound. Immunohistochemical analysis of PrP revealed that the compounds achieved high-specificity labeling (Figs 1b, d and f). The compounds displayed no signal in control sections without amyloid lesions (data not shown).

Similar results were observed in experimental mice. PrP plaques were specifically labeled in brain sections of Tg7 mice infected with the 263K strain, and there was no PrP immunopositive reaction or fluorescence signal in brain sections of uninfected mice (data not shown). We performed *in vivo* experiments using presymptomatic Tg7 mice at a later stage of TSE. A typical image is shown in Fig. 1(g); peripheral administration of BF-168 fluorescently labeled plaques in the cerebral white matter, indicating that the compound efficiently entered the brain and bound to coarse PrP deposits. Subsequent immunostaining verified the specificity and sensitivity for PrP (Fig. 1h). Non-specific staining, such as cerebrovascular labeling, was occasionally observed at 4 h after injection of 5 mg/kg BF-168, but not after 8 h or more. The stability of the fluorescence signals was examined at various time points up to 24 h after injection and the dye–PrP complex remained visible at the latest time. In contrast, there was no significant labeling after an injection of BF-168 into uninfected animals, or after an injection of vehicle alone to terminally ill Tg7 mice. Similar results were obtained for Tga20 mice infected with the RML strain, although plaques were less frequently detected (data not shown).

Anti-prion activity *in vitro*

The anti-prion activities of the compounds were investigated using ScN2a cells, which are most commonly used for drug screening for TSE treatment. Styrylbenzoxazole derivatives, including BF-168, were evaluated and confirmed to inhibit PrPres formation with IC_{50} values in the nanomolar or subnanomolar range (Fig. 2a and Table 1). Styrylbenzothiazole and styrylbenzoimidazole derivatives were similarly potent, in a dose-dependent manner, within a non-toxic dose range (~10 μM) (Table 2). Treatment with vehicle alone showed no inhibitory effect compared with untreated controls (Fig. 2a). We utilized PTA precipitation, which increases the sensitivity of western blotting, and confirmed the potency of BF-168 at a concentration of 10 times the IC_{50}. Furthermore, radiographic film was exposed to the blotted PVDF membranes for 10 times longer than usual before developing. No significant signals were visualized, whereas bands representing the vehicle-treated control were so strong as to be already saturated (Fig. 2b). To determine whether the efficacy was transient, ScN2a cells treated with 10 nM BF-168 were further cultured for 2 weeks in the absence of BF-168. PrPres signals never reappeared, even through four passages after discontinuation of the treatment (Fig. 2c). To exclude the possibility of interference with immunodetection, BF-168 solution at a final concentration of 10 nM was added to a lysate of untreated ScN2a cells before proteinase K digestion. PrP signals were not affected (data not shown). Nor was any alteration observed in cellular PrP level of N2a cells after treatment with 10 nM BF-168 (Fig. 2d).

To investigate whether the efficacy of the compounds depends on pathogen strain, we tested BF-168 in three N2a58 cell lines individually infected with different strains. As shown in Table 3, BF-168 was only effective in N2a58 cells infected with the RML strain, although the inhibitory activity was not as strong as in ScN2a cells (~1 μM). In contrast, BF-168 was ineffective in the same N2a58 cells infected with the 22L or Fukuoka-1 strains up to 10 μM, a dose at which the compound showed host cytotoxicity.

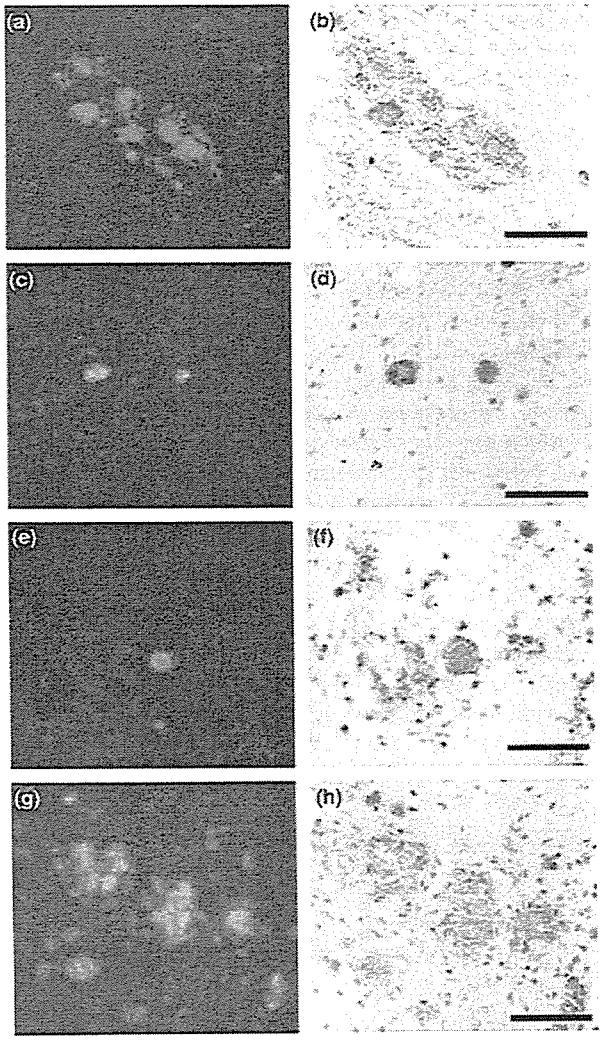

Fig. 1 PrP imaging *in vitro* and *in vivo*. BF-168 fluorescently labeled PrP deposition in a cerebellar section from the case of GSS (a), and in cerebral sections from cases of sporadic CJD with plaques (c) and variant CJD (e). Similar results were obtained from the brains of living TSE-infected mice that were intravenously injected with BF-168 solution (0.5 mg/kg). BF-168 detected PrP deposition in the cerebral white matter between the cortex and hippocampus (g). Sections (a, c, e and g) were subsequently immunoassayed for PrP (b, d, f and h). Bars represent 100 μm (a–f) and 25 μm (g and h).

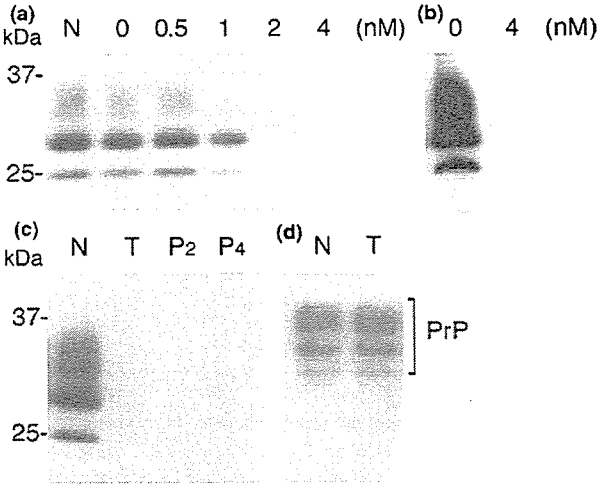

Fig. 2 Effects of BF-168 on PrP expression in ScN2a and N2a cells. BF-168 was added at the designated concentrations to freshly passaged cells. PrPres formation in ScN2a cells was inhibited in a dose-dependent manner (a). To exclude the sensitivity limit of immunoblotting, ScN2a cells treated with 4 nM BF-168 were also analyzed by sodium PTA, and no significant signals were visualized (b). ScN2a cells treated with 10 nM BF-168 were maintained for an additional four passages, and the PrPres signal was not restored in the absence of BF-168 (c). PrP expression was not affected in N2a cells that were grown in the presence of 10 nM BF-168 (d). Lane N, untreated cells; lane 0, cells treated with vehicle alone; lane T, cells treated with 10 nM BF-168; lanes P_2 and P_4, cells following two and four passages after treatment respectively. Bars on the left indicate molecular size markers at 37 and 25 kDa.

Table 3 Anti-prion activities (IC_{50}) of BF-168 in various types of TSE-infected cells

Host cells	Pathogen strains		
	RML	22L	Fukuoka-1
N2a	0.4 nM	None[a]	–[b]
N2a58	~1 μM	None	None
L929	~10 nM	–	–
GT1-7	–	None	–

[a]None, no significant PrPres inhibition up to 10 μM, a dose that affect the rate of cell growth.
[b], not available.

Furthermore, we established L929 cells stably infected with the RML strain. BF-168 inhibited PrPres formation in the RML-infected L929 cells with an IC_{50} in the nanomolar range. We also tested potency against the 22L strain in two other cell lines, N2a and GT1-7 cells. BF-168 was ineffective in either cell line infected with the 22L strain. Other compounds tested here demonstrated similar results (data not shown). These results suggest that the styrylbenzoxazole derivatives exert their inhibitory activity on PrPres formation in a strain-dependent, but not a host cell-dependent, manner.

Therapeutic efficacy *in vivo*

The therapeutic activity of the compounds *in vivo* was assayed in two different mouse models using BF-168 as a representative. Treatment was initiated 2–4 weeks after TSE infection and repeated once a week for 4 weeks. The dosage at a single administration corresponded to a dose sufficient to detect PrP plaques. As shown in Table 4, there was no

Table 4 Effects of BF-168 treatment on intracerebrally TSE-infected mice

Mouse - pathogen strain	*n*	Dose (mg/kg/week)	Administration	Incubation period Mean ± SD (days)
Tg7 - 263K				
	7	Control	-	49.4 ± 1.9
	5	Vehicle	i.v.[a]	50.2 ± 4.1
	5	4	i.v.	52.2 ± 2.6
Tga20 - RML				
	7	Control	-	66.6 ± 1.6
	5	Vehicle	i.v.	64.8 ± 1.6
	5	4	i.v.	72.2 ± 2.5*
	5	10	s.c.[b]	66.0 ± 3.1

* $p < 0.001$ versus the oher groups.

[a]i.V., intravenous injection of BF-168 once a week for 4 weeks from 2 weeks p.i. for Tg7, or 4 weeks p.i. for Tga20.

[b]s.c., continous subcutaneous infusion of BF-168 for 4 weeks from 4 weeks p.i.

significant difference in incubation periods between groups of Tg7 mice infected intracerebrally with the 263K strain, with or without treatment. In contrast, intravenous injection with 4 mg/kg BF-168 significantly prolonged the incubation period (~ 11.4%) of Tga20 mice intracerebrally infected with the RML strain.

In another trial, we used osmotic pumps filled with BF-168 solution, assuming that the route of administration is a key issue. The pump worked continuously for 4 weeks, and the total dosage for the duration was selected to correspond to two to three times that administered intravenously. Subcutaneous infusion of BF-168, however, did not prolong incubation periods of Tga20 mice intracerebrally infected with the RML strain (Table 4). There was no significant difference in incubation period in either group of infected mice between untreated controls and controls treated with vehicle alone.

Discussion

Our results show that styrylbenzoazole derivatives represent candidates for imaging probes as well as therapeutic drugs for TSE. It has been increasingly necessary to develop minimally non-invasive methods for recognizing early clinical infection and evaluating treatment of TSE. We have already focused on two β-amyloid imaging probes and reported them as potential agents for TSE (Ishikawa *et al.* 2004). The problem is, however, that they seemed to have practical limitations because of inadequate brain uptake and washout. Here, we confirmed that novel styrylbenzoazole derivatives clearly labeled PrP plaques *in vitro* and BF-168, the parent compound, entered the brain and labeled PrP plaques *in vivo*, even at a 20-fold lower dose than the probes we previously reported. In brain uptake studies, all of the compounds showed BBB permeability with >1%ID/g, which is proposed to be sufficient for neuroimaging probes. The background staining of 0.5 mg/kg BF-168 was almost absent at 4 h after administration, suggesting excellent clearance from the brain.

Most of styrylbenzoazole derivatives labeled β-amyloid aggregates in AD specimens in this study (data not shown) as well as in the previous study on Alzheimer's (Okamura *et al.* 2004). This is also observed with 2-(1-[6-[(2-fluoroethyl)(methyl)amino]-2-naphthyl]ethylidene)malononitrile (FDDNP), one of the promising agents for imaging β-amyloid deposition. FDDNP has been reported to label PrP plaques in brain sections, and is a candidate for imaging PrP deposition (Bresjanac *et al.* 2003). These findings imply lack of disease specificity, but the compounds should still be useful for some types of TSE, because anatomical distributions of amyloid deposition are characteristically different between diseases. Pathological changes including amyloid deposition of AD brain are always observed in the hippocampus but not in the cerebellum, whereas those of TSE tend to be absent from the hippocampus but to be demonstrated in the cerebellum.

Styrylbenzoazole derivatives detected predominantly PrP plaques, especially in specimens of sporadic CJD with plaques and variant CJD. However, their ability to detect synaptic or perivacuolar PrP deposition remains inconclusive, until more sensitive investigations, such as autoradiography, are available. The compounds tested in this study can be used with radionuclides. ^{18}F-radiolabeled BF-168, which has already been employed for labeling of β-amyloid deposits including both neuritic and diffuse plaques in AD brain (Okamura *et al.* 2004), may be a suitable tool for investigating whether PrP deposition, other than plaque type, can be detected.

This study demonstrated that styrylbenzoazole derivatives have more potent anti-prion activity than the amyloid imaging probes reported previously (Ishikawa *et al.* 2004). Although the neuropathological processes remain unclear, one of the most likely strategies for TSE treatment is a small-molecule drug that can enter the brain and inhibit abnormal PrP formation. It is important to emphasize that styrylbenzoazole derivatives have a wide concentration safety margin, and some were effective even at subnanomolar doses in ScN2a cells. Dozens of drug candidates for TSE have been reported to date but, as far as we know, the most potent inhibitor class for abnormal PrP formation in ScN2a cells is specific blocking antibodies with an IC_{50} in the nanomolar range (Peretz *et al.* 2001).

BF-168 showed no apparent alteration in cellular PrP expression level in N2a cells, and also labeled abnormal PrP deposition both *in vitro* and *in vivo*. These data suggest that styrylbenzoazole derivatives might interact directly with abnormal PrP molecules to block the conversion of normal to abnormal PrP. The structure–activity relationship, examined by introducing side-chain or functional groups into the benzoazole and/or benzene rings, demonstrates that the inhibitory potency is not always the same, even among

closely related compounds (data not shown). Although we could not obtain any insight into inhibitory mechanisms, the efficacy of BF-168 was dependent on pathogen strain, and this is consistent with our previous work using three types of cell lines (Ishikawa *et al.* 2004). In an attempt to further explore strain dependency, we tested three different pathogen strains in one host cell line, and three different host cell lines with one pathogen strain. BF-168 inhibited abnormal PrP formation in all three types of RML-infected cells, including ScN2a cells. By contrast, BF-168 did not demonstrate any inhibitory activity in the 22L- or Fukuoka-1-infected cells. It is well known that prion strains differ in their biological profiles such as the degree of glycosylation and the conformation of PrP molecules. In the imaging experiments we confirmed that the compound bound to a certain type of abnormal PrP aggregates. Thus, it was assumed that the therapeutic efficacy might be based on blocking certain interactions between normal and abnormal PrP, and that BF-168 might recognize the PrP conformation. However, considering a discrepancy in the *in vivo* experiment between PrP imaging and treatment using infected Tg7 mice, these inferences remain unsupported and the precise mechanism of the strain-dependent efficacies needs to be elucidated.

Kocisko *et al.* (2004) reported that anti-prion activity *in vitro* does not always correlate with that *in vivo*. With *in vivo* testing, there are many variables, such as inoculation route, dosing protocol and pathogen strain. The efficacy differed according to the BF-168 administration route in Tga20 mice, even though the dose administered subcutaneously for the same duration was no less than that administered intravenously. This might be due to differences in stability and clearance of BF-168 in relation to the route of administration.

Most previous therapeutic investigations showed a significant benefit *in vivo* when the treatment was started before, or soon after, peripheral TSE infection. Although the efficacy of BF-168 was limited, it is noteworthy that we obtained significant results with peripheral administration at a later stage of the intracerebral infection. In addition, BF-168 showed excellent brain uptake and binding affinity towards PrP aggregates *in vivo*, even at a low dose, suggesting that the compound should be a good imaging probe for clinical use. In the treatment of infected Tga20 mice, BF-168 showed almost the same prolongation of the incubation period but with a 10-fold smaller dose than (trans, trans)-1-bromo-2,5-bis-(3-hydroxycarbonyl-4-hydroxy)styrylbenzene (BSB), which we reported previously as one of the amyloid imaging probes applicable for TSE (Ishikawa *et al.* 2004). BF-168 showed a low IC_{50} of 0.4 nM in treatment of ScN2a cells, whereas the IC_{50} of BSB was more than 1000-fold higher (1.4 μM). We decided the dosing protocol for our experimental animals from *in vitro* data, including the ratio of these IC_{50} values, and from an *invivo* imaging experiment in which 0.1 mg BF-168 per injection was enough to detect PrP deposition. It is also necessary to consider washout of the compound from the brain. Further studies are required to examine issues such as dose–response relationships, administration time and dosing conditions. Furthermore, there was a problem in that administration frequency was limited because animal tail tissue was damaged by repetitive intravenous injections. In addition, it should be investigated whether compounds with slower washout from the brain are more suitable as therapeutic agents.

In conclusion, styrylbenzoazole derivatives efficiently entered the brain and labeled pathological PrP deposition, and demonstrated some anti-prion activities both *in vitro* and *in vivo*. Although their efficacy depended on the pathogen strain, these are a new class of compounds with potential as therapeutic drugs and imaging probes for TSE.

Acknowledgements

This study was supported by grants to KD from the Ministry of Health, Labour and Welfare (H16-kokoro-024) and the Ministry of Education, Culture, Sports, Science and Technology 13557118, 14021085, Japan. The authors thank Dr James W. Ironside of the CJD Surveillance Unit, Edinburgh, UK, for providing the variant CJD specimens.

References

Bresjanac M., Smid L. M., Vovko T. D., Petric A., Barrio J. R. and Popovic M. (2003) Molecular-imaging probe 2-(1-[6-[(2-fluoroethyl)(methyl) amino]-2-naphthyl]ethylidene) malononitrile labels prion plaques *in vitro*. *J. Neurosci.* **23**, 8029–8033.

Brown P., Preece M., Brandel J. P. *et al.* (2000) Iatrogenic Creutzfeldt–Jakob disease at the millennium. *Neurology* **55**, 1075–1081.

Caughey B. and Raymond G. J. (1993) Sulfated polyanion inhibition of scrapie-associated PrP accumulation in cultured cells. *J. Virol.* **67**, 643–650.

Doh-ura K., Mekada E., Ogomori K. and Iwaki T. (2000) Enhanced CD9 expression in the mouse and human brains infected with transmissible spongiform encephalopathies. *J. Neuropathol. Exp. Neurol.* **59**, 774–785.

Fischer M., Rulicke T., Raeber A., Sailer A., Moser M., Oesch B., Brandner S., Aguzzi A. and Weissmann C. (1996) Prion protein (PrP) with amino-proximal deletions restoring susceptibility of PrP knockout mice to scrapie. *EMBO J.* **15**, 1255–1264.

Ishikawa K., Doh-ura K., Kudo Y., Nishida N., Murakami-Kubo I., Ando Y., Sawada T. and Iwaki T. (2004) Amyloid imaging probes are useful for detection of prion plaques and treatment of transmissible spongiform encephalopathies. *J. Gen. Virol.* **85**, 1785–1790.

Kocisko D. A., Morrey J. D., Race R. E., Chen J. and Caughey B. (2004) Evaluation of new cell culture inhibitors of protease-resistant prion protein against scrapie infection in mice. *J. Gen. Virol.* **85**, 2479–2483.

Milhavet O., McMahon H. E., Rachidi W. *et al.* (2000) Prion infection impairs the cellular response to oxidative stress. *Proc. Natl Acad. Sci. USA* **97**, 13 937–13 942.

Nishida N., Harris D. A., Vilette D., Laude H., Frobert Y., Grassi J., Casanova D., Milhavet O. and Lehmann S. (2000) Successful transmission of three mouse-adapted scrapie strains to murine neuroblastoma cell lines overexpressing wild-type mouse prion protein. *J. Virol.* **74**, 320–325.

Okamura N., Suemoto T., Shimadzu H. *et al.* (2004) Styrylbenzoxazole derivatives for *in vivo* imaging of amyloid plaques in the brain. *J. Neurosci.* **24**, 2535–2541.

Okamura N., Suemoto T., Furumoto S. *et al.* (2005) Quinoline and benzimidazole derivatives: candidate probes for *in vivo* imaging of tau pathology in Alzheimer's disease. *J. Neurosci.* **25**, 10 857–10 862.

Peretz D., Williamson R. A., Kaneko K. *et al.* (2001) Antibodies inhibit prion propagation and clear cell cultures of prion infectivity. *Nature* **412**, 739–743.

Prusiner S. B. (1991) Molecular biology of prion diseases. *Science* **252**, 1515–1522.

Race R. E., Caughey B., Graham K., Ernst D. and Chesebro B. (1988) Analyses of frequency of infection, specific infectivity, and prion protein biosynthesis in scrapie-infected neuroblastoma cell clones. *J. Virol.* **62**, 2845–2849.

Race R. E., Priola S. A., Bessen R. A., Ernst D., Dockter J., Rall G. F., Mucke L., Chesebro B. and Oldstone M. B. (1995) Neuron-specific expression of a hamster prion protein minigene in transgenic mice induces susceptibility to hamster scrapie agent. *Neuron* **15**, 1183–1191.

Safar J., Wille H., Itri V., Groth D., Serban H., Torchia M., Cohen F. E. and Prusiner S. B. (1998) Eight prion strains have PrP(Sc) molecules with different conformations. *Nat. Med.* **4**, 1157–1165.

Vorberg I., Raines A., Story B. and Priola S. A. (2004) Susceptibility of common fibroblast cell lines to transmissible spongiform encephalopathy agents. *J. Infect. Dis.* **189**, 431–439.

Will R. G., Ironside J. W., Zeidler M. *et al.* (1996) A new variant of Creutzfeldt–Jakob disease in the UK. *Lancet* **347**, 921–925.

Journal of Pathology
J Pathol 2006; **209**: 484–491
Published online 9 June 2006 in Wiley InterScience
(www.interscience.wiley.com) **DOI:** 10.1002/path.2009

Original Paper

Clusterin expression in follicular dendritic cells associated with prion protein accumulation

K Sasaki,[1]* K Doh-ura,[2] JW Ironside,[3] N Mabbott[4] and T Iwaki[1]

[1] *Department of Neuropathology, Neurological Institute, Graduate School of Medical Sciences, Kyushu University, Fukuoka 812-8582, Japan*
[2] *Division of Prion Biology, Department of Prion Research, CTAAR, Tohoku University School of Medicine, Sendai 980-8575, Japan*
[3] *National CJD Surveillance Unit, University of Edinburgh, Western General Hospital, Edinburgh EH4 2XU, UK*
[4] *Institute for Animal Health, Edinburgh EH9 3JF, UK*

**Correspondence to:*
Dr K Sasaki, Department of Neuropathology, Neurological Institute, Graduate School of Medical Sciences, Kyushu University, Fukuoka 812-8582, Japan.
E-mail: ksasaki@np.med.kyushu-u.ac.jp

Received: 26 January 2006
Revised: 18 March 2006
Accepted: 28 March 2006

Abstract

Peripheral accumulation of abnormal prion protein (PrP) in variant Creutzfeldt–Jakob disease and some animal models of transmissible spongiform encephalopathies (TSEs) may occur in the lymphoreticular system. Within the lymphoid tissues, abnormal PrP accumulation occurs on follicular dendritic cells (FDCs). Clusterin (apolipoprotein J) has been recognized as one of the molecules associated with PrP in TSEs, and clusterin expression is increased in the central nervous system where abnormal PrP deposition has occurred. We therefore examined peripheral clusterin expression in the context of PrP accumulation on FDCs in a range of human and experimental TSEs. PrP was detected immunohistochemically on tissue sections using a novel highly sensitive method involving detergent autoclaving pretreatment. A dendritic network pattern of clusterin immunoreactivity in lymphoid follicles was observed in association with the abnormal PrP on FDCs. The increased clusterin immunoreactivity appeared to correlate with the extent of PrP deposition, irrespective of the pathogen strains, host mouse strains or various immune modifications. The observed co-localization and correlative expression of these proteins suggested that clusterin might be directly associated with abnormal PrP. Indeed, clusterin immunoreactivity in association with PrP was retained after FDC depletion. Together these data suggest that clusterin may act as a chaperone-like molecule for PrP and play an important role in TSE pathogenesis.

Keywords: prion; clusterin; follicular dendritic cell; immunohistochemistry; detergent autoclaving pretreatment; immune deficiency

Introduction

Transmissible spongiform encephalopathy (TSE) is the generic term for the fatal neurodegenerative diseases associated with abnormal prion protein (PrP) deposition in the central nervous system (CNS). Human TSE diseases include Creutzfeldt–Jakob disease (CJD), Gerstmann–Sträussler–Scheinker disease, fatal familial insomnia, and kuru. In cases of variant CJD, transmission is thought to have occurred from exposure to bovine spongiform encephalopathy (BSE)-contaminated meat via the oral route [1–3]. In cases of variant CJD and some animal TSE models, peripheral accumulation of abnormal PrP occurs in the lymphoreticular system, within the lymphoid follicles of spleens, lymph nodes, Peyer's patches, and tonsils [4–6]. In these regions, abnormal PrP accumulates on the surfaces of follicular dendritic cells (FDCs) from an early stage of the disease [7], followed by CNS involvement via the peripheral nervous system [8,9].

Clusterin (apolipoprotein J) is a heterodimeric glycoprotein and is expressed in a variety of mammalian tissues. It is considered to have a variety of functions, including inhibition of complement-mediated cytolysis by binding to the membrane attack complex [10]; regulation of apoptosis [11]; and as a survival factor for germinal centre B cells [12]. We have reported that, during TSE disease, clusterin is associated with deposits of abnormal PrP in the CNS [13]. In the CNS of TSE-affected subjects, clusterin co-localizes with the extracellular plaque-type PrP deposits. Clusterin expression is also up-regulated within lesions of synaptic PrP deposition, even though no co-localization is observed. As clusterin interacts with a range of other molecules [14,15], these findings suggest that secreted clusterin might act as a chaperone-like molecule for PrP. Previous *in vitro* investigations have shown that clusterin is induced in astrocytes by PrP fragments reminiscent of the abnormal PrP isoform [16], and prevents their fibrillar aggregation [17].

FDCs also express clusterin [12]. Therefore we investigated whether clusterin expression in the lymphoreticular system is likewise affected by TSE infection, and associated with the extracellular accumulation of abnormal PrP on FDCs.

Materials and methods

Antibodies

The antibodies used included anti-human PrP C-terminal (rabbit polyclonal, IBL, Japan; raised against a peptide mapping to the C-terminus of human PrP, cross-reacts with mouse PrP), anti-human PrP N-terminal (rabbit, IBL; raised against a peptide mapping to the N-terminus of human PrP, cross-reacts with mouse PrP), anti-human PrP (mouse monoclonal, 3F4, Signet, MA, USA; recognizing amino acid residues 109–112, cross-reacts with hamster PrP), anti-mouse clusterin (goat polyclonal, M-18, Santa Cruz, CA, USA; raised against a peptide mapping to the C-terminus of mouse clusterin), anti-human clusterin (goat, C-18, Santa Cruz; raised against a peptide mapping to the C-terminus of human clusterin), or anti-human clusterin (goat, Chemicon, CA, USA; raised against a purified clusterin from human plasma), anti-mouse CD21/CD35 (CR2/CR1, rat monoclonal, 7G6, PharMingen, CA, USA), anti-human CD35 (CR1, mouse, Ber-MAC-DRC, Dako, Denmark). We assessed two anti-human clusterin antibodies by immunohistochemistry and verified that both gave similar results [13].

Mouse models

Non-transgenic NZW mice and transgenic Tga20 mice [18,19] that express high amounts of mouse PrP were inoculated intraperitoneally (i.p.) with the Fukuoka-1 mouse-passaged scrapie agent strain (NZW/Fu-1, Tga20/Fu-1, respectively). Transgenic Tg7 mice [8,20] that express high amounts of hamster PrP on a mouse-PrP knockout background were inoculated i.p. with the 263K hamster-passaged scrapie agent strain (Tg7/263K). Permission for these animal experiments was obtained from the Animal Experiment Committee of Kyushu University.

Where indicated, C57BL/Dk mice were inoculated either orally or i.p. with the ME7 mouse-passaged scrapie agent strain (C57BL/ME7 mice). To deplete FDCs temporarily, C57BL/Dk mice were given a single i.p. injection of a fusion protein containing the soluble lymphotoxin β receptor domain linked to the Fc portion of human IgG1 (LTβR-Ig) or 100 μg polyclonal human IgG (hu-Ig) (Sandoglobulin®) as a control [21,22]. Where indicated, treatment was given 3 days before (−3 dpi) oral inoculation, or 14 or 42 days after (14 dpi & 42 dpi, respectively) i.p. inoculation with the ME7 scrapie agent strain as described [21,22]. Spleens were analysed 3 days after treatment; Peyer's patches were analysed 70 days after inoculation with the scrapie agent. Mice deficient in interleukin- (IL-) 6 (IL-6-knockout (KO) mice, on a 129/Sv × C57BL/6 background) possess FDC networks but have impaired germinal centres [23]. IL-6-KO mice, and 129/Sv × C57BL/6 immunocompetent wild-type mice, were also inoculated i.p. with the ME7 mouse-passaged scrapie agent strain. Permission for these animal experiments was obtained from the Ethical Review Committee at the Institute for Animal Health, Edinburgh, UK.

Table 1 summarizes the profiles of the mouse lines used in this study.

Human CJD cases

Paraffin-embedded sections of spleens, lymph nodes, appendices, and tonsils were examined from five cases of variant CJD (three males, two females, age range 17–39 years, duration of clinical illness 7–33 months) from the UK National CJD Surveillance Unit, University of Edinburgh, UK. Spleen sections were also examined from four cases of sporadic CJD (two males, two females, age range 55–69 years, duration of clinical illness 4–30 months) from the Department of Neuropathology, Kyushu University. The diagnosis of variant or sporadic CJD was confirmed by postmortem examination. Each case had consent for use of autopsy tissues for research purposes and local Ethics Committee approval for the use of human autopsy tissues from patients with CJD for research was also obtained.

Table 1. Profiles of mouse lines

Line	Background	Modification of PrP expression	PrP^c on FDCs	Reference	Inoculum	PrP^{sc} on FDCs
NZW wild		None	+		Fukuoka-1	+
C57BL/Dk Wild		None	+		ME7	+
Tg7	C57BL/10	MoPrP knockout Overexpress HaPrP under control of the endogenous MoPrP promoter	+	8,20	263K	−
Tga20	129/Sv × C57BL/6	MoPrP knockout Overexpress MoPrP under control of the endogenous MoPrP promoter	−*	18,19	Fukuoka-1	−
IL-6 KO	129/Sv × C57BL/6	None	+	23	ME7	+

MoPrP = mouse PrP; HaPrP = hamster PrP; PrP^c = cellular PrP expression on the FDCs; PrP^{sc} = abnormal PrP accumulation on FDCs of scrapie affected mice; (−) negative; (+) positive.

* Negative on FDCs but some cells within the paracortical T-cell area express PrP^c [19].

The inocula indicated were applied to the respective mouse lines in this study.